

Early Neuronal Loss and Axonal/Presynaptic Damage is Associated with Accelerated Amyloid- β Accumulation in A β PP/PS1 Alzheimer's Disease Mice Subiculum

Laura Trujillo-Estrada^{a,c}, José Carlos Dávila^{a,c}, Elisabeth Sánchez-Mejías^{a,c}, Raquel Sánchez-Varo^{a,c}, Angela Gomez-Arboledas^{a,c}, Marisa Vizuete^{b,c,d}, Javier Vitorica^{b,c,d,*} and Antonia Gutiérrez^{a,c,*}

^a*Department Biología Celular, Genética y Fisiología, Facultad de Ciencias, Instituto de Investigación Biomédica de Málaga (IBIMA), Universidad de Málaga, Spain*

^b*Department Bioquímica y Biología Molecular, Facultad de Farmacia, Universidad de Sevilla, Spain*

^c*Centro de Investigación Biomédica en Red sobre Enfermedades Neurodegenerativas (CIBERNED), Spain*

^d*Instituto de Biomedicina de Sevilla (IBIS)-Hospital Universitario Virgen del Rocío/CSIC/Universidad de Sevilla, Spain*

Handling Associate Editor: Javier S. Burgos Muñoz

Accepted 10 April 2014

Abstract. The progressive cognitive decline leading to dementia in Alzheimer's disease (AD) patients is the consequence of a severe loss of synapses and neurons affecting particular cell subpopulations in selected brain areas, with the subiculum being one of the earliest regions displaying severe atrophy and pathology. The lack of significant neuronal loss in most AD models is, in fact, the major shortcoming for the preclinical evaluation of drugs that could have greater potential in patients to alleviate or prevent this disease. In this study, using immunohistochemical and stereological approaches, we have analyzed the histopathological events in the subiculum of A β PP751SwedLondon/PS1M146L mice, a transgenic model that displays neuronal vulnerability at early ages in hippocampus and entorhinal cortex. Our results indicate that the subiculum is the earliest affected region in the hippocampus, showing a selective early loss of both principal neurons (28%) and SOM-positive interneurons (69%). In addition, our data demonstrate the existence of an early axonal and synaptic pathology, which may represent the beginning of the synaptic disruption and loss. These neurodegenerative processes occur in parallel, and closely related, with the onset and accelerated progression of the extracellular amyloid- β deposition, thus suggesting plaques as major contributors of neuronal/axonal damage. Data reported here indicate that this AD model displays a selective AD-like neurodegenerative phenotype in highly vulnerable regions, including the subiculum, and therefore can be a very useful model for testing the therapeutic ability of potential compounds to protect neurons and ameliorate disease symptoms.

Keywords: Alzheimer's disease, amyloid- β plaques, axonal damage, hippocampus, neuronal loss, subiculum, transgenic mice

*Correspondence to: Javier Vitorica, Departamento de Bioquímica y Biología Molecular, Facultad de Farmacia, Universidad de Sevilla, 41012 Sevilla, Spain. Tel.: +34 955923053; Email: vitorica@us.es; Antonia Gutiérrez, Departamento de Biología Celular, Genética y Fisiología, Facultad de Ciencias, Universidad de Málaga, 29071 Málaga, Spain. Tel.: +34 952133344; E-mail: agutierrez@uma.es.

¹These authors are co-senior authors.

INTRODUCTION

The progressive cognitive decline that ultimately leads to dementia in Alzheimer's disease (AD) is consequence of a severe loss of synapses and neurons that selectively affects particular cell subpopulations in brain areas critical for learning and memory [1–6]. Although transgenic mice, based on the overexpression of proteins harboring one or several mutations found in familial AD, progressively develop amyloid- β (A β) deposits and tau hyperphosphorylation, along with dystrophic neurites and activated astrocytes and microglia, very limited or no neuronal death has been reported in vulnerable brain areas of these AD models [7–10]. This lack of significant neuronal loss is, in fact, the major shortcoming of AD models for the preclinical evaluation of drugs that could have greater potential in patients to alleviate or prevent this disease. Therefore, the characterization of the neurodegenerative phenotype of AD models is a critical step in ensuring success for translating therapeutic efficacy.

The hippocampal formation, a key structure of the medial temporal lobe memory system and one of the earliest regions to be affected in AD, consists of a number of subdivisions including the dentate gyrus, the hippocampus proper (areas CA1 and CA3), the entorhinal cortex, and the subiculum [11–13]. Marked neuronal reduction occurs in the hippocampal formation of AD patients [14–21]. Even in mild AD, a marked neuronal loss can be found in the entorhinal cortex and hippocampus [2, 4], and these changes result in decreased volume of these brain areas [22, 23]. Unlike most transgenic animal models, which do not exhibit the neurodegenerative spectrum of disease observed in the patient population, in the A β PP751SweLondon/PS1M146L (A β PP/PS1) mice we have previously reported a selective and significant neuronal loss in the hippocampus proper, dentate gyrus, and entorhinal cortex. Subpopulations of GABAergic interneurons were selectively affected at early ages in hippocampal CA fields and dentate gyrus [24, 25] as well as entorhinal cortex [26]. However, pyramidal neurons were first affected in entorhinal cortex [26] and then later in CA1 hippocampus [27], similarly to the pathological pattern described in patients [2, 28, 29]. The loss of these neurons was associated with the prominent extracellular amyloid pathology along with the age-dependent increase in the soluble oligomeric A β content and/or the induced cytotoxic inflammatory response [27, 30].

In contrast to the rest of the hippocampal formation, the subiculum has received comparatively little

investigation in the AD field. The subiculum is the principal target of the CA1 pyramidal cells and serves as the major output structure of the hippocampal formation to widespread subcortical and cortical areas (for review, see [31]). In AD patients, the subiculum is among the earliest regions displaying severe atrophy and pathology [1, 16, 18, 32–37]. Loss of the subicular neurons has been reported to be associated with clinical AD [19, 21]. Thus, damaged hippocampal–cortical and hippocampal–subcortical communication might be significant for the memory impairment seen in patients. In AD models, tremendous attention has been focused on hippocampal (CA fields and dentate gyrus) pathology, however very few studies comment specifically on subiculum neurodegeneration so far [38, 39].

Here we have characterized the histopathological events in the subiculum of the A β PP751SweLondon/PS1M146L model by immunohistochemistry and stereological approaches to detect changes in the number of neurons. Our data indicate that the subiculum is the earliest affected hippocampal region showing a selective loss of both principal cells and SOM-positive interneurons at an early age (4–6 months) in parallel with an early onset of extracellular amyloid deposits and prominent axonal damage. The most relevant feature of this model is the selective AD-like neurodegenerative phenotype in highly AD-vulnerable regions. Therefore, this model can be very useful for testing the therapeutic ability of potential compounds to protect neurons and ameliorate disease symptoms due to this neurodegenerative phenotype.

MATERIALS AND METHODS

Animals

Male transgenic mice expressing familial AD-causing mutations in the A β PP and PS1 genes were used in this study [40]. The bigenic mice were obtained by crossing homozygous mice expressing human mutant PS1M146L (under HMG-CoA reductase promoter) to hemizygous mice expressing human mutant A β PP751 carrying the Swedish (KM670/671NL) and London (V717I) mutations (under the control of the Thy1 promoter). Mice represented F6–F10 offspring of heterozygous transgenic mice. Non-transgenic mice (WT) of the same genetic background (C57BL/6) and age were also used. All animal experiments were carried out in accordance with the European Union regulations (Council Directive 86/609/ECC of November 24th, 1986) and approved by the committee of

animal use for research at Malaga University, Spain (RD 1201/2005 of October 10th, 2005).

Tissue preparation

After deep anesthesia with sodium pentobarbital (60 mg/kg), 2, 4, 6, 12 and 18-month-old, A β PP/PS1, PS1, and WT mice ($n=6$ /age/genotype) were perfused transcardially with 0.1 M phosphate-buffered saline (PBS), pH 7.4 followed by 4% paraformaldehyde, 75 mM lysine, 10 mM sodium metaperiodate in 0.1 M phosphate buffer (PB), pH 7.4. Brains were then removed, post-fixed overnight in the same fixative solution at 4°C, cryoprotected in 30% sucrose, sectioned at 40 μ m thickness in the coronal plane on a freezing microtome, and serially collected in wells containing cold PBS and 0.02% sodium azide (each series contained sections that represented 1/7th of the total brain).

Immunohistochemistry

Serial sections from A β PP/PS1, PS1, and WT mice were assayed simultaneously for light and confocal microscopy immunohistochemistry using same batches of solutions to minimize variability in immunolabeling conditions as previously reported [24–26, 41]. Free-floating sections were first pre-treated with 3% H₂O₂/3% methanol in PBS pH 7.4 for 20 min to inhibit endogenous peroxidase, and then with avidin- biotin Blocking Kit (Vector Labs, Burlingame, CA, USA) for 30 min to block endogenous avidin, biotin and biotin-binding proteins. For single immunolabeling, sections were incubated overnight at room temperature with one of the following primary antibodies: anti-somatostatin (SOM) goat polyclonal (1:1000 dilution; Santa Cruz Biotechnology); anti-parvalbumin (PV) rabbit polyclonal (1/5000 dilution, Swant); anti-human amyloid- β protein precursor (hA β PP) rabbit polyclonal (1/20000; Sigma) or goat polyclonal (1/20000; Meridian life sciences); anti-A β mouse monoclonal 6E10 (1:1500 dilution; Sigma); anti-A β ₄₂ rabbit polyclonal (1/5000; Millipore); anti-oligomeric A β (OC) rabbit polyclonal (1/5000; Millipore); anti-synaptophysin (Syn) rabbit polyclonal (1:1000 dilution; Abcam); anti-MAP-2 rabbit polyclonal (1/5000 dilution; Chemicon); anti-neurofilament rabbit polyclonal (1/5000 dilution; Chemicon), anti-VGluT1 guinea pig polyclonal (1/10000 dilution; Chemicon); anti-VGAT guinea pig polyclonal (1/5000 dilution; Calbiochem); anti-LC3 rabbit polyclonal (1/1000 dilution; Cell Signaling);

anti-ubiquitin rabbit polyclonal (1/5000 dilution; Dako); anti-phospho-tau (AT8) mouse monoclonal (1/250 dilution; Pierce); anti-cathepsin D (Cat-D) goat polyclonal (1/100 dilution; Santa Cruz Biotechnology); anti-choline acetyltransferase (ChAT) goat polyclonal (1/1000 dilution; Millipore) over 24, 48, or 72 h at room temperature. To retrieve intracellular A β , sections were pre-treated for 7 min with 85% formic acid before incubation with the anti-A β antibodies. For general antigen retrieval method sections were previously heated at 80°C for 20 min in 50 mM citrate buffer pH 6.0. The tissue-bound primary antibody was detected by incubating with the corresponding biotinylated secondary antibody (1:500 dilution, Vector Laboratories), and then followed by 1:2000 streptavidin-conjugated horseradish peroxidase (Sigma Aldrich). The peroxidase reaction was visualized with 0.05% 3-3'-diaminobenzidine tetrahydrochloride (DAB), 0.03% nickel ammonium sulphate, and 0.01% hydrogen peroxide in PBS. Specificity of the immune reactions was controlled by omitting the primary antisera. After DAB, some immunolabeled sections were incubated 3 min in a solution of 20% of Congo red. Sections were then mounted onto gelatin-coated slides, dehydrated in graded ethanol, cleared in xylene and coverslipped with DPX (BDH) mounting medium.

For double A β ₄₂/Cat-D, A β ₄₂/hA β PP, A β ₄₂/Syn, hA β PP/SOM, or hA β PP/VGluT1 immunofluorescence labeling, sections were first sequentially incubated with the indicated primaries antibodies followed by the corresponding Alexa488/568 secondary antibodies (1:1000 dilution; Invitrogen). Sections were examined under a confocal laser microscope (Leica SP5 II).

For pyramidal cell discrimination, we used a 5 \times immunohistochemical approach previously reported [26]. Sections were first and sequentially incubated with the following interneuron markers: anti-SOM goat polyclonal (1:1000, Santa Cruz), anti-Calretinin (CR) rabbit polyclonal (1:5000 dilution; Swant), anti-VIP rabbit polyclonal (1:5000 dilution, Acris), anti-PV rabbit polyclonal (1/5000 dilution, Swant) as described above. After the DAB-nickel reaction (dark blue end product), sections were then incubated 3 days with the neuronal marker anti-NeuN monoclonal antibody (1:1000 dilution; Chemicon). The second immunoperoxidase reaction was developed with DAB only (brown reaction end product). The appropriate controls were performed to avoid any false positive immunostaining due to cross-reactivity between detection systems. To clearly discriminate the different streptavidin-

peroxidase reactions, the first one (for interneurons) was always developed with DAB-nickel (dark blue) solution whereas the second one (NeuN) only with DAB (light brown). Moreover, the different compartment localization of interneuron (cytoplasm) and NeuN (nuclei) epitopes completely guarantee the correct non-overlapped visualization of both reactions and the interpretation of the results.

Thioflavin-S staining

Free-floating sections were incubated for 5 min with 0.015% Thio-S (Sigma) in 50% ethanol, and then washed in 50% ethanol, in PBS, mounted onto gelatin coated slides and coverslipped with 0.1 M PBS containing 50% glycerin and 3% triethylenediamine.

Plaque loading quantification

Plaque loading was defined as percentage of total subicular area stained for A β . Quantification of extracellular A β content was performed as previously reported [26]. Thioflavin-S staining was examined under an Olympus BX-61 epifluorescent microscope using FITC filter and 4 \times objective. Images were acquired with an Olympus DP71 high-resolution digital camera using the Cell-A program (Olympus). The camera settings were adjusted at the start of the experiment and maintained for uniformity. Digital images (4 sections/mouse) from 2, 4, 6, and 12-month old A β PP/PS1 mice ($n=4/\text{age}$) were analyzed using Visilog 6.3 analysis program (Noesis, France). The plaque area (Thioflavin-S positive) within the subiculum was identified by level threshold which was maintained throughout the experiment for uniformity. The color images were converted to binary images with plaques. The subicular area in each 4 \times image was manually outlined. The plaque loading (%) for each transgenic mouse was estimated and defined as (sum plaque area measured/sum subicular area analyzed) \times 100. The sums were taken over all slides sampled and a single plaque burden was computed for each mouse. The mean and standard deviation (SD) of the plaque loading were determined using all the available data. Quantitative comparisons were carried out on sections processed at the same time with same batches of solutions.

Plaque size morphometric analysis

Four coronal sections stained with Thioflavin-S from 2 ($n=5$), 4 ($n=5$), 6 ($n=5$), and 12-month-old

($n=5$) A β PP/PS1 mice were analyzed using the nucleator method with isotropic probes by the NewCAST software package from Olympus stereological system. Subiculum was analyzed using a counting frame of 6022.8 μm^2 and step length of 173.53 μm . For individual plaque measurement, a 40 \times objective was used. Number of plaques/ mm^2 falling into four surface categories (ranging from <200 μm^2 to >2000 μm^2) was calculated. Each analysis was done by a single examiner blinded to sample identities.

Stereological analysis

Immunopositive cells for SOM, PV, or NeuN belonging to the different animal groups (WT, PS1, and A β PP/PS1) and ages (2, 4, 6, 12, or 18 months) were quantified ($n=5-6/\text{age}/\text{group}$). Briefly, the quantitative analyses were performed using an Olympus BX61 microscope interfaced with a computer and a Olympus DP71 digital camera, and the NewCAST (Computer Assisted Stereological Toolbox) software package (Olympus, Denmark). The number of neurons was quantified in every 7th section (with a distance of 280 μm between sections) through the rostrocaudal extent of the subiculum (between -2.46 mm anterior and -4.60 mm posterior to Bregman coordinates, according to the atlas of Franklin and Paxinos [42]). An average of 6-7 sections was measured in each animal. The subicular area was defined using a 4 \times objective and the number of neurons was counted using a 100 \times /1.35 objective. We used a counting frame of 902.52 μm^2 with step lengths of 46.98 μm for SOM and 95 μm for NeuN counting. The numerical density (ND; cells/ mm^3) was estimated using the following formula: $\text{ND} = Q/(\Sigma A * h)$, where 'Q' is the number of disector-counted somatic profiles, ' ΣA ' is the area of the counting frame, and 'h' is the height of the optical disector (10 μm). The precision of the individual estimations is expressed by the coefficient of error (CE) [43] calculated using the following formula: $\text{CE} = 1/Q \times (3A - 4B + C/12) / 2$, where $A = \Sigma Q_i$, $B = \Sigma Q_i \times Q_{i+1}$, $C = \Sigma Q_i \times Q_{i+2}$. The CEs ranged between 0.07 and 0.1. An investigator who was blind to the experimental conditions (age, genotype, and marker) performed neuronal profile counting.

Co-localization analysis

Double immunopositive subicular cells for A β_{42} and Cat-D or for A β_{42} and hA β PP were analyzed to determine the extent of colocalization between both couple of markers in 2 month-old A β PP/PS1

animals. Confocal images of $1,024 \times 1,024$ pixels were acquired by using a Leica SP5 II confocal microscope and a $40\times$ objective. A total of 30 (A β_{42} /Cat-D) to 50 (A β_{42} /hA β PP) cells were randomly photographed ($n=3$). Laser settings were adjusted at the start of the experiment and maintained for uniformity. Images were analyzed using LAS AF Lite program (Leica). For A β_{42} /Cathepsin-D quantification we considered the number of A β_{42} points that were cathepsin-D positives. For A β_{42} /hA β PP quantification, we determined the area of A β_{42} which co-localized with hA β PP.

Electron microscopy

Fixed brains (see above) from 4–6 month-old mice were sectioned at $50\ \mu\text{m}$ or $250\ \mu\text{m}$ thickness in the coronal plane on a vibratome (Leica VT1000S) and serially collected in wells containing cold PB and 0.02% sodium azide. For standard electron microscopy, the $250\ \mu\text{m}$ -thick sections were postfixed in 1% osmium tetroxide in 0.1 M PB, block stained with uranyl acetate, dehydrated in acetone, and flat embedded in Araldite (EMS, USA). Selected areas were cut in ultrathin sections and examined with an electron microscope (JEOL JEM1400).

For the immunogold labeling, the $50\ \mu\text{m}$ sections were first washed with PBS and incubated in a 50 mM glycine solution 5 min in order to increase the antibody binding efficiency. Following the standard immunohistochemical protocol, the tissue was incubated 48 h in primary rabbit polyclonal antibody anti-A β (1/5000; Millipore) in a PBS 0.1M/0.02%Tx-100/1% BSA solution at 22°C. Then, sections were washed in PBS, and incubated with 1.4 nm gold-conjugated goat anti-rabbit IgG (1:100; Nanoprobes) overnight at 22°C. After postfixing with 2% glutaraldehyde and washing with 50 mM sodium citrate, the labelling was enhanced with the HQ SilverTM Kit (Nanoprobes), and gold toned. Finally, the immunolabeled sections were processed as above by the osmium fixation, dehydration and embedding steps. In negative control experiments, the primary antibody was omitted.

Statistical analysis

Data was expressed as mean \pm SD. The comparison between two mice groups (WT and A β PP/PS1 mice or PS1 and A β PP/PS1 transgenic mice) was done by two-tailed *t*-test, and for comparing several groups (WT, PS1, and A β PP/PS1 mice) and ages, we used one-way ANOVA, followed by Tukey *post-hoc* multiple comparison test (SigmaStat[®] 2.03, SPSS Inc).

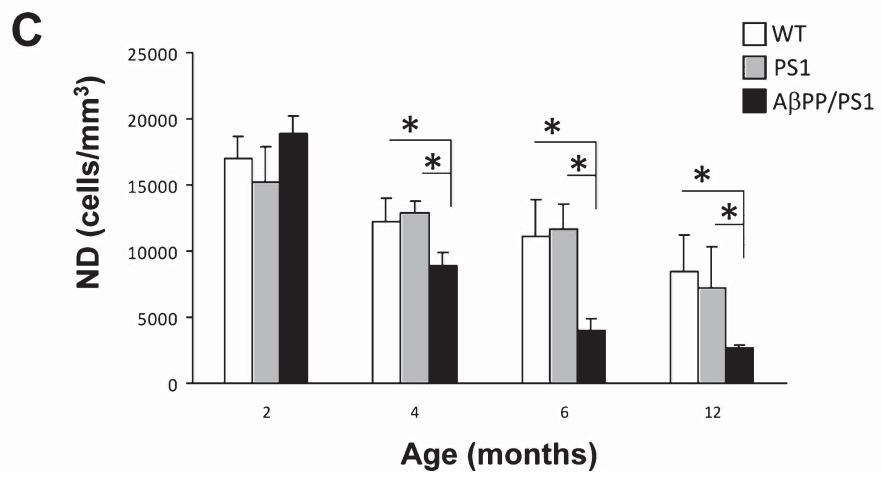
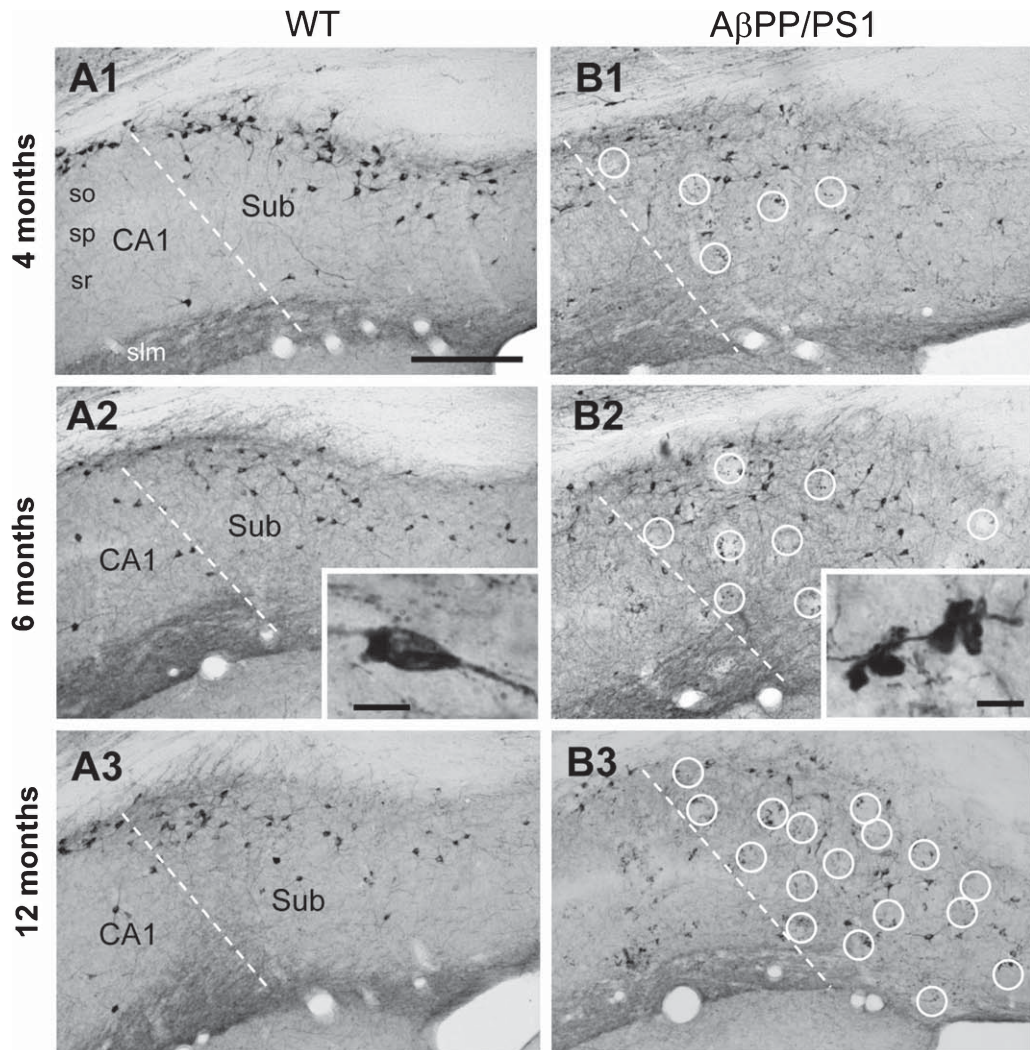
In both cases, the significance was set at 95% of confidence.

RESULTS

Selective loss of subicular interneurons at early ages

We have first determined the numerical density of SOM-immunostained neurons in the subiculum (including pro-subiculum) of A β PP/PS1 at 2, 4, 6 and 12 months of age and compared to age-matched PS1 and WT mice. The initial immunohistochemical analysis showed that the majority of subicular SOM-containing cells were located in the deep pyramidal cell layer and in the polymorphic layer (Fig. 1A1–A3). These interneurons (see inset in Fig. 1A2), corresponding to O-LM cells of hippocampal sector CA1, innervate the distal apical dendrites of pyramidal neurons in the outer molecular layer which receives the main excitatory input from layer III of the medial entorhinal cortex. WT and PS1 animals displayed a similar pattern of SOM-immunolabeling. However, A β PP/PS1 mice (Fig. 1B1–B3) showed a reduced number of labeled somata since early ages (4–6 months) and the presence of numerous SOM-positive dystrophic neurites (see inset in Fig. 1B2), mostly located around amyloid plaques. The stereological study (Fig. 1C) demonstrated a significant decrease ($27.17 \pm 8.50\%$, Tukey $p < 0.05$) in the numerical density (neurons/ mm^3) of SOM-positive cells in A β PP/PS1 mice at 4 months of age compared to age-matched WT group. This decrease was much more marked at 6 months of age ($69.37 \pm 8.53\%$, Tukey $p < 0.05$). No further decrease was detected at 12 month-old ($69.15 \pm 3.05\%$, Tukey $p < 0.05$). PS1 group did not show changes respect to WT group at any age tested. These data were in line with our previous reports showing a significant loss of SOM interneurons in the hippocampus proper (CA1–CA3 and dentate gyrus) and entorhinal cortex of our A β PP/PS1 model at 6 months of age [25, 26].

We have also analyzed whether another major interneuron population, the cells expressing the calcium binding protein parvalbumin (PV) which include basket and axo-axonic GABAergic neurons, was also early affected in the subiculum of our AD model. PV-positive interneurons were present throughout the principal cell layer of the subiculum (Fig. 2A–B). We have not found significant differences in the numerical density (Fig. 2C) of this GABA population at 6 months of age between A β PP/PS1 (8415.58 ± 1429.79) and



WT (10721.93 ± 3057.86) mice and neither at the advanced age of 18 month-old (7556.79 ± 1033.90 versus 9136.28 ± 1205.44 for A β PP/PS1 and WT mice, respectively). Moreover, and unlike SOM-cells, the neuronal population positive for PV did not develop dystrophic neurites with the progression of age. In fact, even the PV-immunopositive processes and somata that were located in the very near proximity of amyloid plaques displayed a normal morphology (see Fig. 2B2).

These findings indicated that in the subiculum of this AD model the SOM interneurons, but not the PV-cells, were highly vulnerable at the initial stages of the disease and that the degenerative process of the SOM population preceded the observed in the hippocampus and entorhinal cortex.

Loss of subicular principal neurons at early ages

Though in this AD model the loss of hippocampal principal neurons is a late event (17–18 months of age) [27, 44], in the entorhinal cortex pyramidal neurodegeneration begins at an early age (6 months) [26]. Therefore, we next examined whether subicular principal neurons were also affected early by determining their numerical density at 2 and 6 months of age in comparison with age-matched PS1 and WT animals. To specifically distinguish principal cells from interneurons, we have performed a multiple immunoperoxidase labeling approach as previously reported ($5 \times$ immunolabeling) [26]. Principal cells were discriminated by a single NeuN-nuclei labeling in light brown color whereas interneurons (those expressing SOM/PV/CR/VIP alone or in combination) displayed also a dark-blue cytoplasmic labeling (see Fig. 3 and for details see insets).

As shown in Fig. 3, the microscopic observation of the $5 \times$ immunolabeled sections at 2 and 6 months of age revealed no qualitative differences in the immunostaining pattern and cell distribution between A β PP/PS1 and PS1 or WT animals. Small rounded areas devoid of cells and characterized by the presence

of dystrophic neurites (in this case only GABAergic dystrophies), which corresponded to areas occupied by amyloid plaques, were easily detected in A β PP/PS1 animals, few plaques at 2 months (Fig. 3A3) and more numerous at 6 months of age (Fig. 3B3), as expected. The quantitative stereological study (Fig. 3C) revealed a significant ($-28.04 \pm 11.76\%$; $p < 0.05$) principal cell loss in A β PP/PS1 mice (compared to PS1 and non-transgenic littermates) at 6 months of age. No differences were detected at 2 months of age. These data demonstrated that principal subicular neurons were vulnerable at early ages and the first hippocampal pyramidal neurons to be affected by the course of the disease.

Accelerated intra- and extracellular A β accumulation in the subiculum

Considering the toxic effect of A β accumulation on neuronal survival we next investigated the temporal intra/extracellular expression of A β in the subiculum of the double transgenic model from 2 to 12 months of age by A β_{42} immunohistochemistry (Fig. 4). Similar results were obtained with the OC antibody for the oligomeric forms of A β (results not shown). As shown in the panoramic images (Fig. 4A–C), the subiculum is one of the earliest forebrain regions to express and accumulate A β . At 2 months of age the presence of intracellular A β was clearly seen in subicular neurons which presented a strong punctuate immunolabeling (Fig. 4A, D, and for a detail see inset in D). We did not check in younger animals, but most probably the intracellular A β accumulation in subiculum started before 2 months of age. The formation of extracellular A β deposits was also first observed in this area at 2 months of age; however the number of plaques was really low indicating that the onset of extracellular amyloid pathology was at the initial stage. At 4 months, numerous plaques were already formed in the subiculum (Fig. 4E) and further on the number and size of these deposits significantly increased, as shown here for 6 and 12 months of age (Fig. 4F and G, respectively). As

Fig. 1. Significant reduction of subicular SOM-interneurons in A β PP/PS1 mice at early ages. Light microscopy images of SOM immunoreactivity in the subiculum of WT (A1–A3) and A β PP/PS1 (B1–B3) mice at 4, 6 and 12 months of age. SOM-positive neurons were located in the deep pyramidal cell layer and in the polymorphic layer (an immunoreactive neuron is shown at higher magnification in A2 inset). A decrease in the number of immunoreactive somata was observed in A β PP/PS1 mice. Abundant immunoreactive dystrophic neurites (higher magnification detail is shown in B2 inset) were seen associated to amyloid plaques (indicated with open white circles) in the double transgenic mice. The number of dystrophies clearly increased with age. Stereological quantification (C) of SOM-positive neurons in WT, PS1, and A β PP/PS1 mice at 2, 4, 6 and 12 months of age ($n = 4$ per genotype and age). Results showed a significant decrease in the density of SOM-immunoreactive somata (cells/mm³) in A β PP/PS1 mice compared to WT-PS1 since 4 months of age. Data (mean \pm SD) was analyzed by one-way ANOVA $p < 0.01$ ($F(14,24) = 24,3$), followed by Tukey *post-hoc* multiple comparison test. Significance ($*p < 0.05$) was indicated in the figure. No differences were detected between PS1 and WT animals. Scale bars, A1–A3 and B1–B3, 200 μ m; insets 14 μ m.

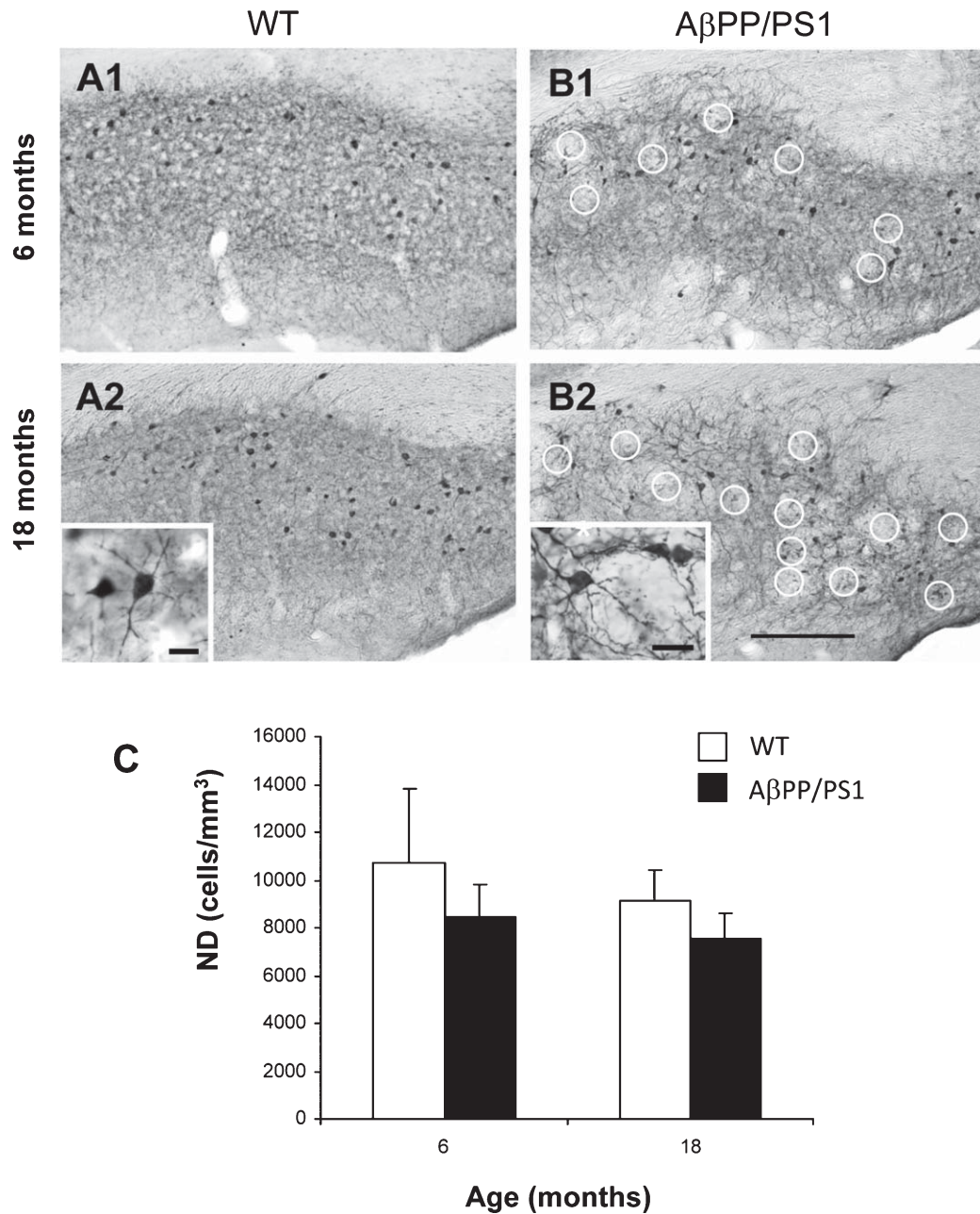


Fig. 2. PV-interneurons are resistant to neurodegeneration in A β PP/PS1 subiculum. Light microscopy images of PV immunoreactivity in the subiculum of WT (A1 and A2) and A β PP/PS1 (B1 and B2) at 6 and 18 months of age. No changes were detected between both genotypes in the number and morphology of these inhibitory neurons. Immunolabeled PV-neurons are shown at higher magnification in A2 inset. PV-neurons located near A β plaques in A β PP/PS1 mice displayed normal morphology as shown in B2 inset. Open white circles indicate areas occupied by A β plaques (not stained) in A β PP/PS1 subiculum. Stereological quantification (C) of PV-positive neurons (cells/mm³) at 6 and 18 months of age in WT and A β PP/PS1 mice revealed no significant differences between the genotypes at the two ages examined. Scale bars, A1, A2, B1 and B2, 200 μ m; insets 14 μ m.

rapidly increased the extracellular accumulation of A β the presence of intraneuronal A β in the somata tended to decrease. In fact, it was really difficult to distinguish A β -positive somata at light microscopy from 6 months

onward due to the high amount of extracellular amyloid deposits occupying the subiculum.

To quantitatively compare the extracellular amyloid progression with age in the subiculum with other

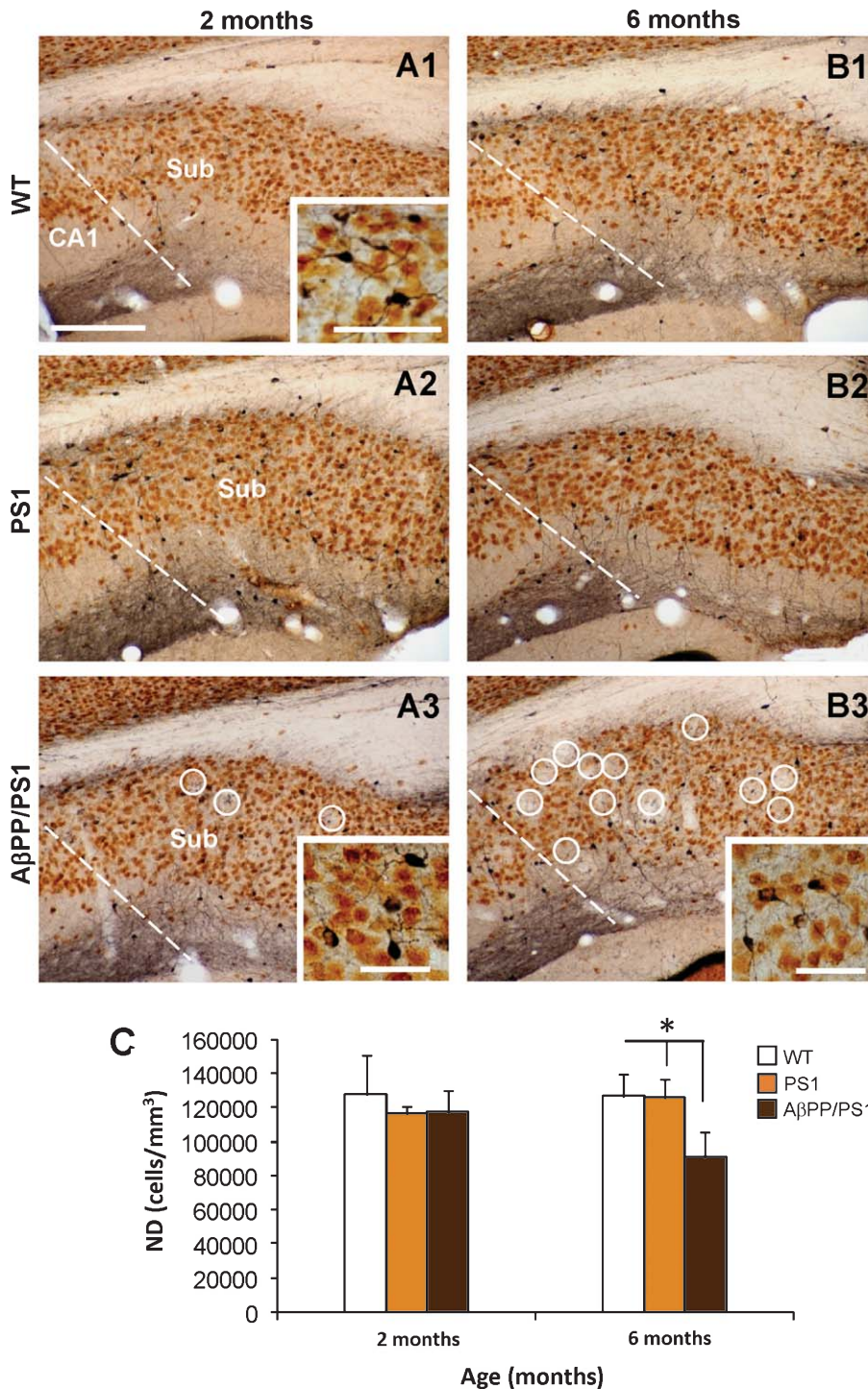


Fig. 3. Loss of principal neurons in the A β PP/PS1 subiculum at early ages. Multiple 5 \times (SOM, PV, CR, VIP and NeuN)-immunolabeling in the subiculum, of WT (A1 and B1), PS1 (A2 and B2), and A β PP/PS1 (A3 and B3) mice at 2 and 6 months of age. Principal neurons (single NeuN-labeled cells in brown color) were immunohistochemically differentiated from interneurons (SOM/PV/CR/VIP-labeled cells in dark blue color) as seen in the higher magnification images of the insets. Stereological counts (C) of principal cells revealed a significant (two tailed *t*-test, $p < 0.05$) decrease in the density (neurons/mm³) of this cell population in the A β PP/PS1 subiculum compared to age-matched WT or PS1 mice at 6 months of age. No differences were found at 2 months of age. Data are given as mean + SD. Open white circles indicated amyloid plaques location in the A β PP/PS1 subiculum. Scale bars, A1–A3 and B1–B3, 200 μ m; insets in A1 and A3, 100 μ m; inset in B3, 50 μ m.

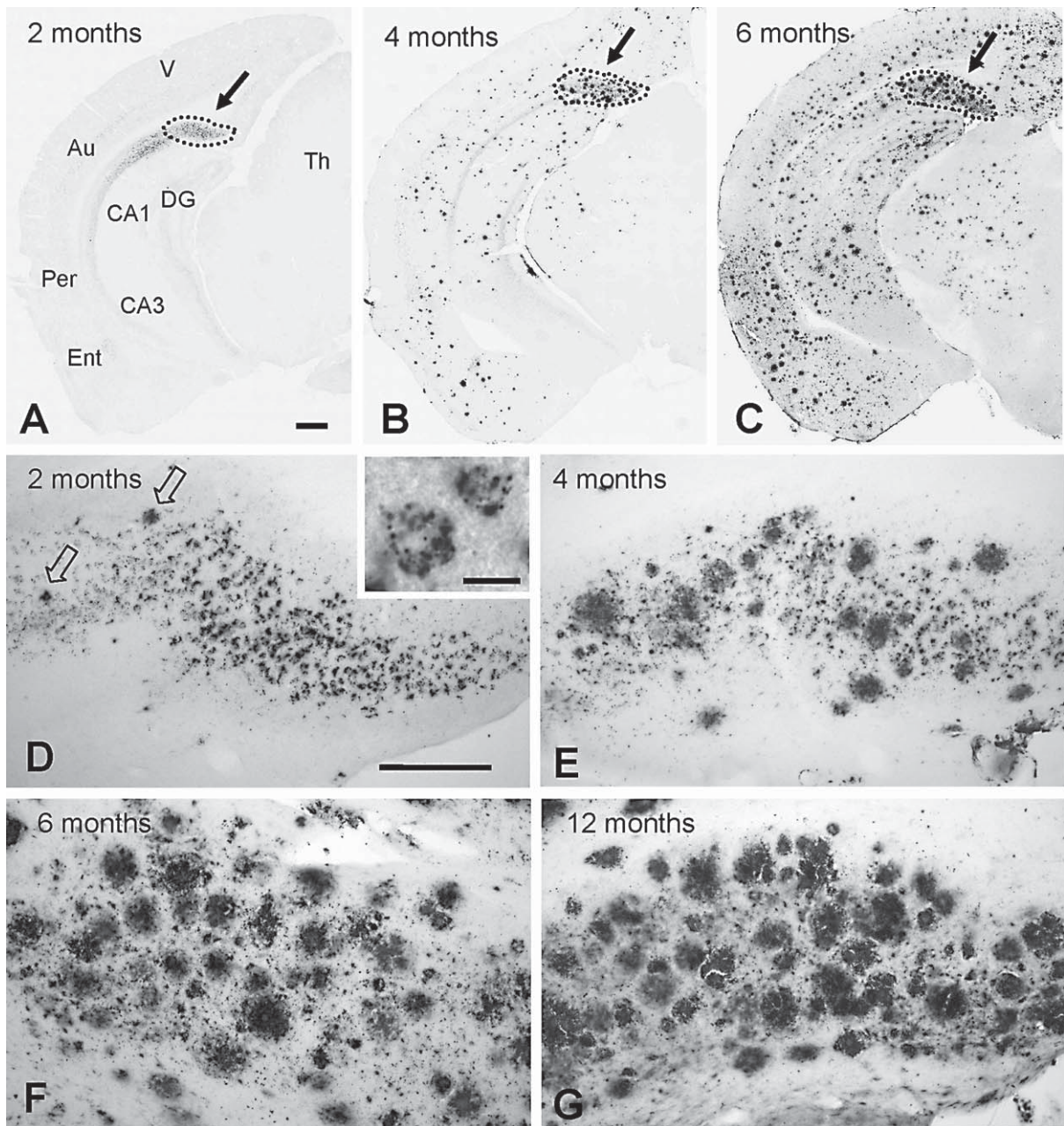


Fig. 4. Early accelerated intra- and extracellular A β accumulation in the A β PP/PS1 subiculum. A β_{42} immunohistochemistry at 2 (A and D), 4 (B and E), 6 (C and F), and 12 (G) months of age. A–C, panoramic views of the caudal telencephalon showing the A β_{42} immunoreactivity in the subiculum (dashed area pointed with a black arrow) compared to other hippocampal and cortical areas from 2 to 6 months. Intracellular A β appears as early as 2 months and neurons show a punctate labeling suggestive of a vesicular location (inset in D). Abundant A β plaques were already seen at 4 months of age and plaques progressively increased, in number and size, with age. CA1, CA3, hippocampal subfields; DG, dentate gyrus; Ent, entorhinal cortex; Per, perirhinal cortex; Au, auditory cortex. Scale bars, A–C, 500 μ m; D–G, 200 μ m; inset in D 10 μ m.

highly vulnerable brain areas, such as CA1 and entorhinal cortex, we have measured the area occupied by the A β deposits (plaque loading) in these brain regions using Thioflavin-S stained sections (images not shown). Thioflavin-S labeled only extracellular A β and allowed

better image analysis quantification of plaques since intracellular A β pool was excluded. As shown, the subiculum (Fig. 5A) is the earliest and most severely affected area by the extracellular amyloid pathology. The subicular amyloid load was $0.06 \pm 0.1\%$ and

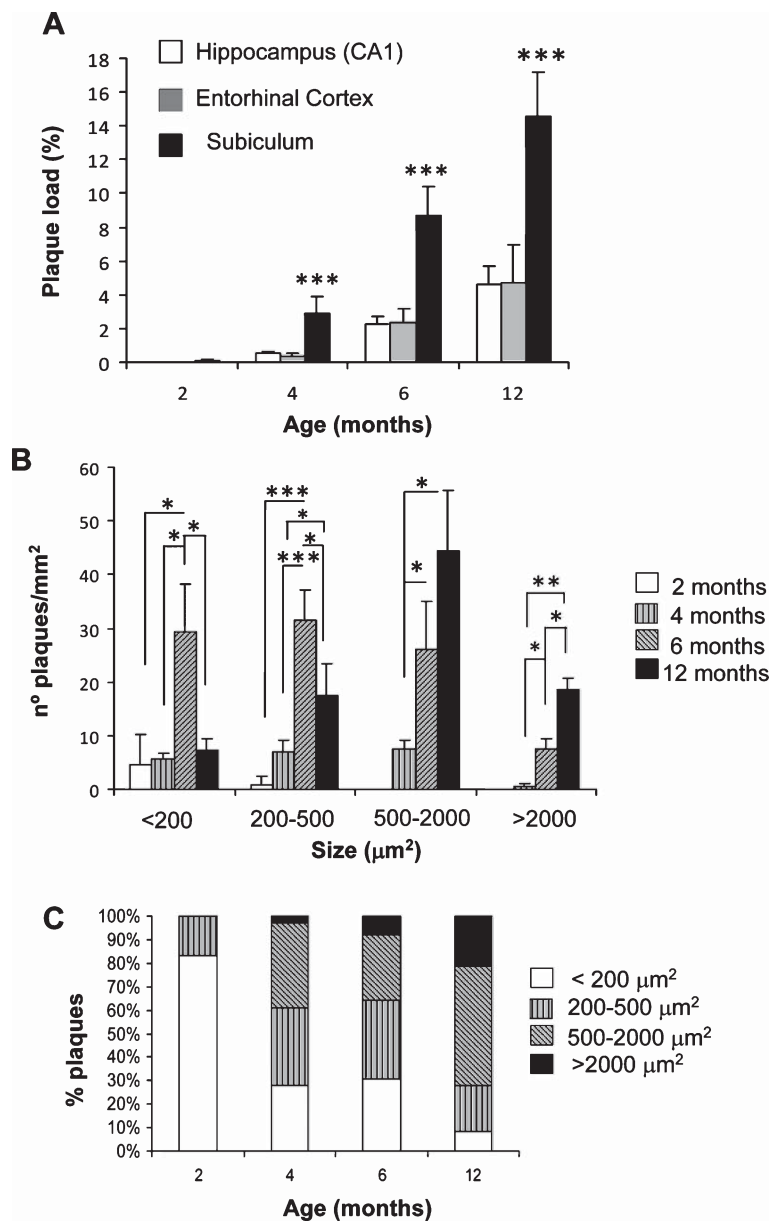


Fig. 5. A β load and plaque progression with age in A β PP/PS1 subiculum. A) A β load in subiculum rapidly increased with age and it was significantly higher than in CA1 and entorhinal cortex at all ages analyzed. B, C) The number (plaques/mm²) and the size (μm^2) of the A β plaques in the subiculum exhibited a marked increase with age (two tailed *t*-test, **p* < 0.05, ***p* < 0.01, ****p* < 0.001).

$2.77 \pm 1.17\%$ at 2 and 4 months of age, respectively. A β deposition increased to $8.67 \pm 1.70\%$ at 6 months of age and reached to $14.57 \pm 0.63\%$ at 12 months (the maximum was at 18 months with $25.31 \pm 4.10\%$, not shown). A β load was significantly greater in subiculum than in CA1 and entorhinal cortex at all ages analyzed. At 4 months of age, the subicular amyloid deposition was markedly accelerated and reached up to 5 times higher than in CA1 and 7 times than in entorhinal cor-

tex. Then after, at 6 and 12 months, the plaque load in subiculum, was between 3–4 times higher than in CA1 or entorhinal cortex. Therefore, the subiculum showed the greatest age-related A β load and also exhibited the earliest neuronal loss.

The age-dependent increase in the total amyloid load in the subiculum appeared to be associated with both the number and size of the plaques. To support this observation, we next determined the plaque density

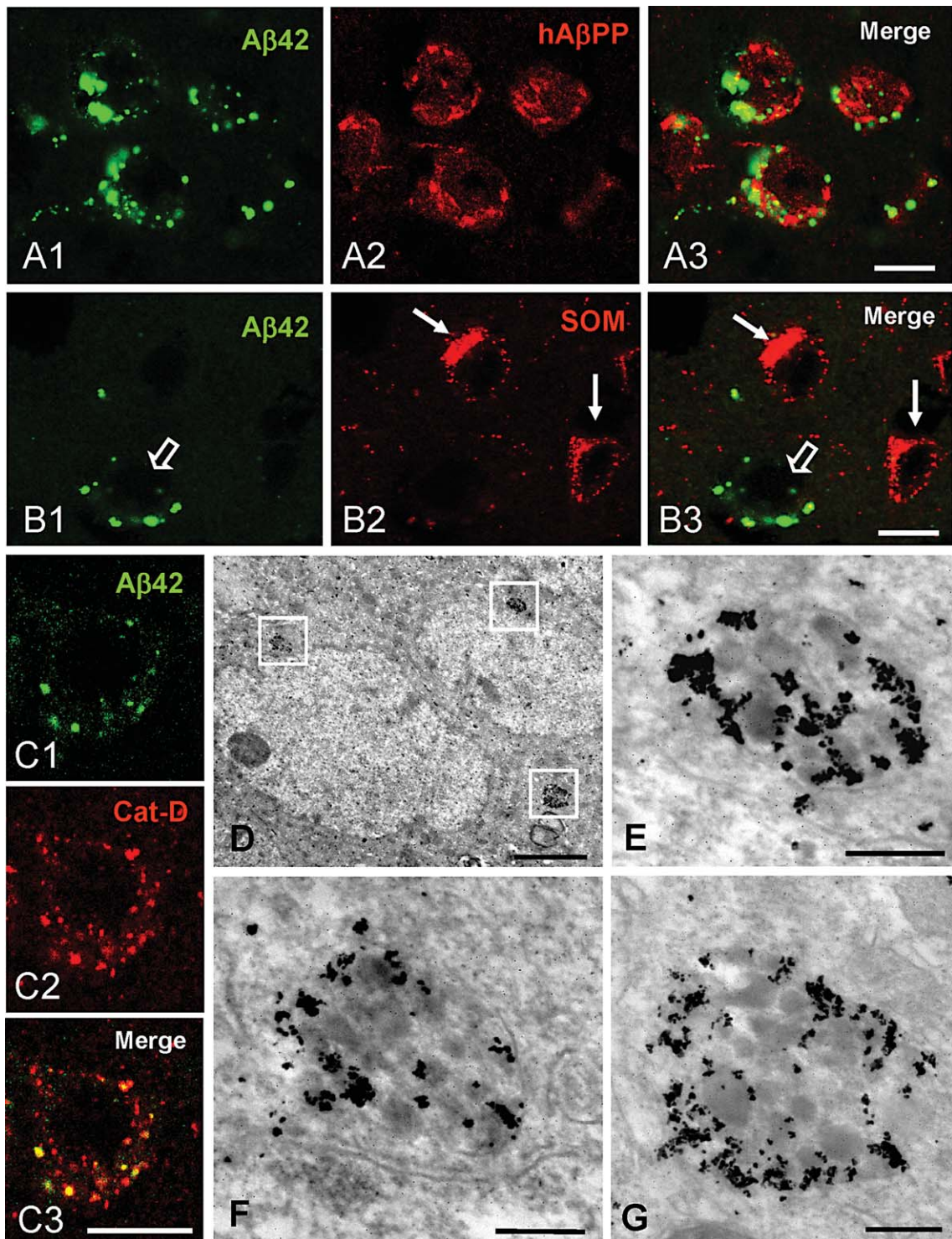


Fig. 6. Intracellular A β is mostly localized in lysosomal vesicles of principal cells. Double confocal immunofluorescence labelings show the presence of A β in A β PP-positive (principal) neurons (A1–A3) but not in SOM-interneurons (B1–B3). Most A β ₄₂ was localized in lysosomal vesicles as shown by double A β ₄₂/Cathepsin-D labeling and confocal microscopy (C1–C3). A β immunogold electron microscopy reveals the restricted subcellular location of A β within endolysosomal organelles of principal neuronal cell bodies. Scale bars: A–C, 10 μ m; D, 2 μ m; E–G, 0.2 μ m.

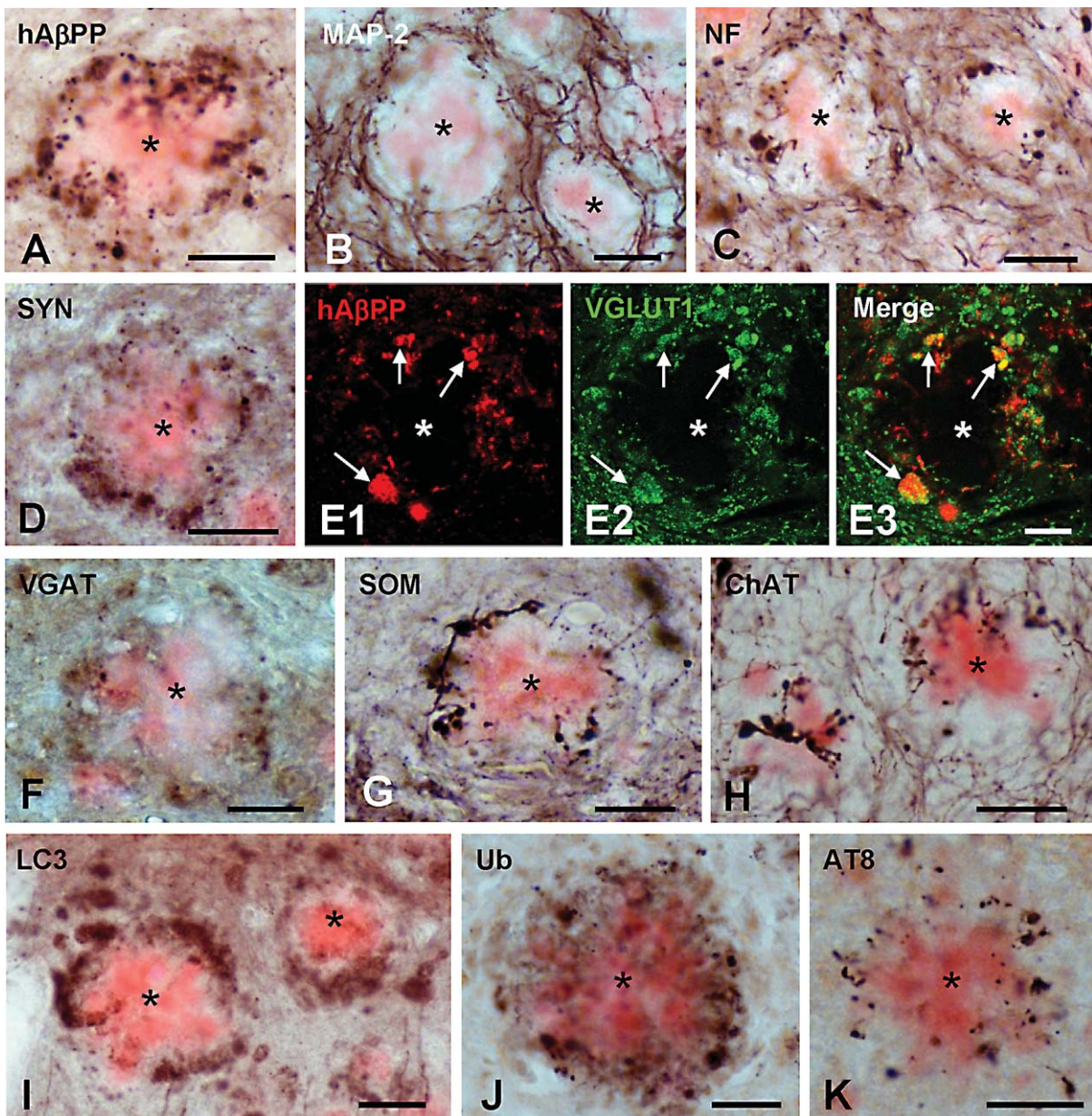


Fig. 7. A β plaques are closely surrounded by axonal/synaptic dystrophies containing phospho-tau and autophagy vesicles. A) A β plaque (Congo red-stained) surrounded by numerous dystrophic neurites immunopositive for hA β PP antibody. B) Dystrophic neurites were not immunopositive for MAP-2 (dendritic marker). C) Immunoreactivity for neurofilament (axonal marker) was found in dystrophic neurites surrounding plaques. D) Plaque associated dystrophies were immunoreactive for synaptophysin (synaptic marker). E1–E3) Confocal double immunofluorescence labeling for hA β PP (red) and VGLUT1 (green) shows extensive co-localization (arrows) of the two markers indicating the axonal/synaptic glutamatergic nature of hA β PP-positive dystrophic neurites around plaques. F–H) Congo red-stained plaques were surrounded by axonal/synaptic dystrophies immunopositive for VGAT (marker for GABAergic terminals), somatostatin (marker for a GABAergic subpopulation) and ChAT (cholinergic marker). I–K) Dystrophies around plaques were immunolabeled for the autophagy marker LC3, ubiquitin and phospho-tau (AT8). Asterisks indicate A β plaques. Scale bars: A–D and F–K, 25 μ m; E1–E3, 10 μ m.

(plaque/mm²) dissected into four size categories ranging from <200 μ m² to those >2000 μ m² (Fig. 5B), as well as the percent of each plaque category (Fig. 5C), at 2, 4, 6 and 12 months of age. The appearance of

plaques in this region began at 2 months of age and they were mostly under 200 μ m², and then progressively increased in number at 4 months with the formation also of bigger plaques. However, the most significant

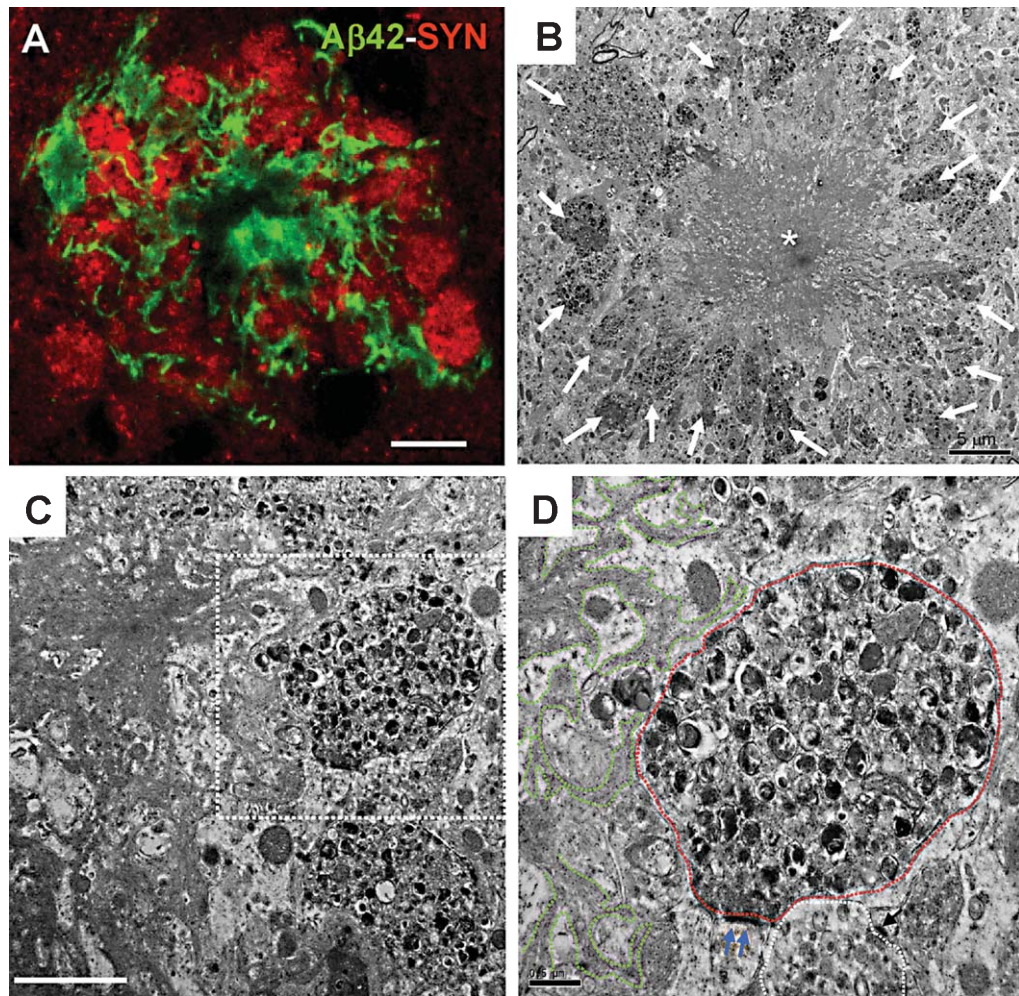


Fig. 8. Tight association between extracellular A β and synaptic dystrophies. A) Double confocal A β_{42} (green) and synaptophysin (SYN, red) labelling show how A β threads from a plaque closely cover SYN-positive dystrophies. B) Electron microscopy micrograph of an A β plaque (asterisk) surrounded by numerous dystrophic neurites (white arrows). C) An electron microscopy image of the plaque periphery showing dystrophic neurites in close contact with A β threads. D) is a higher magnification image of the squared area in C; a dystrophic presynaptic terminal (outlined with red line), contacting with a normal postsynaptic element (postsynaptic density is pointed with blue arrows), is in the very close proximity of A β threads (outlined in green color). Scale bar: A, 10 μ m; B, 5 μ m; C, 2 μ m; D, 0.5 μ m.

increase in the number of plaques/mm² was at the age of 6 months for each size category (5, 4.6, 3.4, and 14.5 times higher than at 4 months for those plaques <200, 200–500, 500–2000, and >2000 μ m², respectively, $n=5$, two tailed t -test, $p<0.05$), with the most abundant being those at <500 μ m². Interestingly, at 12 months the plaque distribution switched and the predominant plaque size was >500 μ m². Then our data demonstrated that the number of plaques significantly build-up with age, but most remarkable, plaque size also displayed a striking increment.

Since intraneuronal A β accumulation precedes amyloid plaque formation in the subiculum, we further

investigated the A β expression in subicular neurons as a potential toxic agent to induce the neurodegeneration. The early presence of intraneuronal A β in A β PP-positive cells was confirmed by double A β_{42} /hA β PP immunofluorescence labeling (Fig. 6A1–A3) in 2-month-old A β PP/PS1 mice. These A β PP-positive cells corresponded to principal neurons since the mutated human A β PP transgene is expressed only by this population in the transgenic mice used. It can be argued then that this early accumulation of A β within principal cells could be responsible of their vulnerability. However, SOM-positive interneurons were also highly affected at early ages, and these

cells did not accumulate intracellular A β (Fig. 6B1–B3), since they do not express the mutated human A β PP. Therefore, it is very unlikely that the neuronal loss in the subiculum, at least for interneurons, was induced by the intracellular A β .

As shown here, the labeling of A β_{42} and hA β PP just marginally overlaps in the same subcellular compartments. In fact, only $3.36 \pm 1.79\%$ ($n=30$ cells) of A β_{42} co-localized with hA β PP. This demonstrated the specificity of the A β antibody, since it does not cross-react with the A β PP antibody and that hA β PP processing and A β accumulation should take place in different intracellular compartments. In this sense, the punctuate labeling of the A β_{42} antibody was suggestive of vesicular location. Several studies have reported the preferential location of A β in vesicles of the endosome-lysosome system [38] including autophagy vesicles [41, 45]. Confocal images of double A β_{42} /cathepsin-D labeling (Fig. 6C1–C3) indicated that most of the A β was in fact associated with lysosomal structures in the somata of the principal subicular neurons. Quantitative analysis demonstrated that $88.9 \pm 18.2\%$ ($n=50$ cells) of the intracellular A β_{42} labeling co-localized with cathepsin-D. Thus, A β is accumulated preferentially in lysosomal vesicles. Furthermore, immunogold electron microscopy experiments demonstrated a restricted location of A β within endolysosomal subcellular compartments of the principal neuronal somata (Fig. 6D–G). Immunogold labeled organelles displayed an electron-dense granular content typical of endolysosomes (see higher magnification images in Fig. 6E–G).

A β plaques as inductors of early axonal/presynaptic pathology in the subiculum

The pathogenic mechanisms leading to neuron loss in AD have not been completely elucidated yet, and the extracellular amyloid deposits could be major contributors for neuronal damage/loss. In our model, the hippocampal plaques are surrounded by numerous dystrophic neurites of axonal/presynaptic origin [41, 45]. Then, we next examined the dystrophy pathology in the subiculum and its association with amyloid plaques using light and electron microscopy approaches. The formation of plaques in the subiculum was paralleled with the appearance of dystrophic neurites in their very close periphery. The hA β PP antibody is a well-established marker for dystrophies (Fig. 7A), and in our model labeled dystrophies belonging to glutamatergic cells as we show here with the double labeling A β PP/VGLUT1 (see Fig. 7E1–E3). While

no dystrophic dendrites around plaques were detected with MAP2 immunostaining (Fig. 7B), numerous dystrophic neurites were labeled with different axonal/synaptic markers such as NF (Fig. 7C), synaptophysin (Fig. 7D), VLGUT1 (Fig. 7E2), and VGAT (Fig. 7F). In addition, we observed SOM-positive (7G) or ChAT-positive (7H) axonal dystrophies surrounding subicular plaques. Altogether, these data confirmed the axonal origin of the dystrophies that surround plaques in the subiculum.

We and others have reported the accumulation of autophagy vesicles within dystrophies [41, 45–47]. This abnormal collection of vesicles belonging to the autophagy-lysosome degradation system might result from a defective cytoskeleton-mediated transport. We have next checked whether subicular dystrophies displayed immunoreactivity for LC3 (autophagy marker), ubiquitin (marker for protein degradation), and AT8 (phosphorylated tau). As shown in Fig. 7 (I–K), these axonal dystrophies were strongly labeled with all these markers suggesting a focalized altered microtubule vesicular transport that compromise protein degradation with the subsequent accumulation of vesicles and un-degraded proteins that disrupts axonal structure.

A direct toxic effect of the A β plaques on surrounding axons might be the cause of dystrophic formation. In fact, the confocal microscopy evaluation of double A β_{42} /synaptophysin labeling (Fig. 8A) revealed a very close spatial association between both markers with the extracellular A β encircling, almost wrapping, the synaptophysin-positive dystrophies. For a better resolution, we next evaluated this tight association between plaque and dystrophies at the transmission electron microscopy (Fig. 8B–D). Figure 8B shows a typical amyloid plaque in this model (neuritic plaque), completely surrounded by numerous dystrophic neurites. In their periphery, plaques gave off many long branches coming in close contact with the dystrophies (Fig. 8C, D). Dystrophies were morphologically characterized by the presence of multiple heterogeneous autophagy-like vesicles, as expected.

The early axonal defects in the subiculum of this AD model could directly affect presynaptic terminals. Though the plaque-associated dystrophies were labeled with the synaptic marker synaptophysin, this labeling could be due to the abnormal accumulation of this protein along the axon due to transport failure, and not to be present in synaptic boutons. However, electron microscopic examination revealed that presynaptic terminals were indeed dystrophic (Fig. 8D) and displayed abnormal morphology with huge collection of autophagy/lysosomal vesicles. Though these

dystrophic terminals made contact with normal post-synaptic elements their function and viability could be somehow compromised.

These data demonstrated the existence of an early axonal/synaptic pathology in the subiculum of this AD model that may represent the beginning of synaptic disruption and loss.

DISCUSSION

Neuron loss is the best anatomopathological substrate that correlates with cortical atrophy and dementia during disease progression in AD. However, most transgenic animals do not display this fundamental degenerative feature of patients. To evaluate the effectiveness of potential neuroprotective therapies for AD, it is essential that animal models exhibit neuronal damage/dysfunction, and even most importantly neuronal death, relevant to the disease in vulnerable brain regions and cell populations. The present work provides new evidence and further support our previous studies [24–27, 30, 41, 45] on the selective AD-like neurodegenerative phenotype of the A β PP751SweLondon/PS1M146L model (data summarized in Table 1). We show here that the subiculum of this model is the earliest affected hippocampal region exhibiting a wide repertoire of AD-like pathological manifestations including 1) accelerated A β accumulation, both intra- and extracellularly; 2) prominent axonal neuritic pathology, that affects presynaptic terminals, with the accumulation of autophagy vesicles, and 3), and most valuable, significant neuronal loss from principal and local inhibitory populations.

As we have reported previously, this A β PP/PS1 transgenic model has the advantage over other models of showing significant loss of neurons in highly vulnerable brain areas [24–26] similar to AD patients. Loss of interneurons was an early event (4–6 months of age) in the hippocampal CA subfields and dentate gyrus, as well as in the entorhinal cortex, however principal neurons were differentially affected by age in these areas. While the entorhinal principal neurons showed early vulnerability (6 months of age) the hippocampus (CA1 subfield) displayed significant pyramidal cell decline only at old ages (>17 months of age). Few others transgenic models have also been reported to have neuronal death [39, 48–51], however this was usually quantitatively minor and/or occurred at very late ages. Subicular neurodegeneration has been previously reported in the 5xFAD model at 9 months of age [38, 39]. Nevertheless, in these studies no quantita-

tive analysis was made to determine the extent of subicular cell loss and neither the vulnerable neuronal type was identified. Here we demonstrate by unbiased stereology a significant decline in SOM-containing interneurons (–27% and –69% at 4 and 6 months of age, respectively) and, most importantly, in principal subicular neurons (–28% at 6 months) of our A β PP/PS1 model at early ages. Therefore, this is the first study showing a quantitative decline of subicular neurons, and noteworthy, occurring as early as 4–6 months of age. Together, and of relevance, subiculum is the first hippocampal brain region exhibiting principal neuronal loss in this model.

Among the potential causative agents for this neuronal loss, A β is the leading candidate in amyloidogenic models bearing familial mutations, as the A β PP/PS1 model used in this study. In fact, A β pathology in the subiculum preceded the loss of neurons. Furthermore, we have also compared the severity of the amyloid pathology in the subiculum with other highly AD vulnerable brain areas, such as CA1 of hippocampus and entorhinal cortex. Interestingly, the subiculum displayed up to 5 and 7 fold increased A β load than CA1 and entorhinal cortex, respectively, at the age of 4 months. Therefore, subiculum is the earliest and most severely affected region by the amyloid pathology. In consequence, we also observed an extensive neuronal (pyramidal and GABAergic) degeneration in this particular brain region.

Abundant intraneuronal accumulation of A β ₄₂ was seen at 2 months of age mostly located in the endolysosomes and immediately after a rapid onset of amyloid plaques was manifested. As the plaque load increased with age the intracellular A β labeling was less evident. In fact, at 6 months of age it was really difficult to visualize A β -immunolabeled neuronal somata at light microscopy suggesting a possible transient localization of A β in the neuronal compartments (soma versus axonal/synaptic?). However, immunogold labeling demonstrated the presence of some intracellular A β within the cell bodies at least in 6-month-old A β PP/PS1 mice. We cannot rule out the possibility that plaques bind most A β antibodies thus preventing the intracellular A β labeling. Our results are in agreement with others since A β pathology (intra preceding extra) was reported to be early present in the subiculum of other transgenic models [38, 39, 52].

As to which A β (intra or extra) mainly contributes to the neuronal death in this region, our data point to the extracellular pool as the most likely toxic agent. Interneurons do not express the human mutant A β PP transgene in our A β PP/PS1 model (see Fig. 6),

Table 1
Summary of the major neuropathological findings in the A β PP751SweLondon/PS1M146L transgenic model

	Subiculum	Hippocampus (CA1) *	Entorhinal Cortex**
Intracellular A β	2 mo	2 mo	NT
Extracellular A β	2-3 mo	4 mo	4 mo
Dystrophic neurites	2-3 mo	4 mo	4 mo
Neuronal loss	4 mo (SOM+) 6 mo (pyramidal)	4 mo (CR+) 6 mo (SOM+) 18 mo (pyramidal)	6 mo (SOM+and pyramidal)
Neuroinflammation	3-4 mo	4-6 mo (microglial M2 phenotype) 18 mo (microglial M1 phenotype)	6 mo (microglial M2 and M1 phenotypes)

The age (months, mo) when intracellular A β (immunoreactivity with the A β ₄₂ or oligomer-specific OC antibodies), extracellular deposits (immunopositive for 6E10, A β ₄₂, or OC antibodies, or stained with thioflavin-s or congo red), dystrophic neurites around plaques (immunopositive for A β PP, SYN, ubiquitin, LC3, or phospho-tau AT8 antibodies), neuronal loss (measured by stereological analysis of SOM+, CR+or pyramidal neurons), and neuroinflammation (microglial and astroglial activation) are detected is indicated. NT, non detected. SOM+, immunopositive somatostatin interneurons; CR+, immunopositive calretinin interneurons. *Data from references [24, 25, 27]. **Data from reference [26].

therefore these cells do not produce and accumulate A β , ruling out the possibility of the intraneuronal source as the causative agent for the death in the SOM-population. On the other hand, principal subicular neurons contain intracellular A β at an early age (2 months or even before), and though the present results do not allow us to completely discard the toxic role of this intracellular stock, the loss of this population (approximately 30%) is delayed until the age of 6 months. Thus, it is most likely to be associated with the accelerated extracellular A β accumulation. This asseveration was also based on: 1) early (2 months) intracellular A β accumulation is seen in CA1 principal neurons of our model (see Fig. 4 A,D), however no neuronal loss in the CA1 pyramidal layer is detected until 17-18 months of age [27, 44]; 2) principal cell loss in the entorhinal cortex is also an early event (6 months) in this model, however it is associated with extracellular rather than intracellular A β pathology [26]. In fact, the vulnerable principal neurons in the entorhinal cortex were those located in the highly A β loaded deep layers (V-VI) and interestingly, these cells did not even expressed the human A β PP transgene and therefore did not accumulate A β intracellularly; 3) early intracellular A β has been detected in many other animal models, however neuronal loss is usually absent or occurred at late ages [7-10]; 4) A β plaques are a potent source of neurotoxic damage as many axonal dystrophies developed in their close periphery (neuritic plaques); 5) A β plaques induce a strong glial activation in subiculum (data not shown) as seen in hippocampus and entorhinal cortex [26, 27]. A cytotoxic profile of this inflammatory response was temporally associated with the pyramidal neuronal death in these brain regions.

Therefore, cerebral amyloidosis (extracellular) seems to be the driving force for neuronal loss and the axonal/synaptic damage in the subiculum as well

as in other brain areas [24-26, 30, 41, 45]. Amyloid plaques are potentially major sources of soluble and toxic oligomeric A β [53]. Then, the accelerated and severe formation of plaques in subiculum, compared to other brain regions, could locally increase the concentration of these oligomers since early ages affecting the most vulnerable neuronal populations.

Subicular A β deposits were surrounded by hyperphosphorylated tau-positive axonal dystrophies and A β oligomers have been shown to induce an increase in tau hyperphosphorylation [54, 55] as well as axonal transport failure with organelle accumulation through GSK3 β signaling [45, 56]. In support of this idea, we have recently demonstrated the involvement of A β oligomers in the activation of GSK3 β and tau phosphorylation [30]. Together, A β oligomers released from plaques might cause locally the interruption of axonal transport leading to a severe accumulation of vesicles mostly from autophagy pathway (LC3-positive) due to failed lysosome maturation [41, 45] (present work) and in consequence the formation of axonal dystrophies. These dystrophies are positive for synaptic proteins (synaptophysin or VGluT1) as shown by confocal microscopy which might reflect synaptic protein accumulation due to axonal transport deficiency. Alternatively, some (or most) dystrophies might be actually presynaptic boutons directly affected by the plaque-associated toxic A β oligomers. In agreement with the last suggestion, we have demonstrated by electron microscopy the presence of dystrophic synaptic terminals making contact with normal postsynaptic elements near plaques in subiculum as we have previously shown also in CA1 [41]. These morphologically altered synaptic terminals might represent the initial step of axonal degeneration previous to the synapse loss, the major correlate for cognitive deficits in the initial stages of the disease [1, 3, 5, 6]. In addition,

axonal/synaptic damage could trigger a neurodegenerative process toward the cell bodies. In line with this, we and others have reported a relationship between extracellular A β accumulation in axonal fields and the progressive degeneration of their away located projecting neurons in AD models [24, 57]. This suggestion is also supported by the apparent resistance of the PV positive GABAergic cells. As shown in this and previous work, the number of subicular, hippocampal, and entorhinal PV positive cells was not modified in the A β PP/PS1 model. These data are in line with the relative resistance of these cells observed in AD patients [58, 59]. Furthermore, at the age tested, the PV positive cells developed few (if any) dystrophic neurites even in close proximity to the A β plaques (see Fig. 2B2). At present, we do not know the mechanisms that determine the relative protection of this neuronal subpopulation to the A β pathology. However, it is possible that the high expression of a Ca²⁺-chelating protein, such as PV, could protect the cell from the extracellular A β damage.

Altogether, our data support A β plaques as major contributors of neuronal/axonal damage in this AD model. The relevance of this conclusion for the disease in humans could be of controversial since no clear association has been made so far between the extent of amyloid burden and dementia severity in AD patients. Moreover, A β deposition begins over a decade prior to the dementia and asymptomatic cortical A β deposition in elderly individuals is also well documented [60–64]. However, a recent report [65] has shed light on this intriguing topic and discriminate demented and non-demented individuals with high amyloid burden on the basis of their neuropathological phenotype. Authors identified that plaques in demented cases had significant higher amount of oligomeric A β and, importantly, a higher number of dystrophic neurites compared to non-demented individuals. In addition, accumulation of phospho-tau into synaptic compartments, and stronger glial activation response discriminated demented from non-demented cases. These findings highlight the existence of different plaques, in relation to their toxicity, that might account for the onset and severity of dementia during disease progression. Therefore, the characterization of plaques on the basis of their capacity to induce axonal and neuronal damage is crucial to validate animal models for research and drug testing. In this sense, our A β PP/PS1 model is of great interest since these mice develop human-like neuritic plaques whose toxicity can be modulated *in vivo*, as we have recently shown, by lithium administration resulting in a marked reduc-

tion of neuronal and axonal damage and cognitive improvement [66].

The subiculum is the main hippocampal output, and therefore hippocampal–cortical and hippocampal–subcortical communication arises most predominantly from subicular neurons [12, 13]. In fact, this region is specifically involved in spatial memory and navigation, as well as in stress responses and limbic-mediated affective, cognitive, and behavioral processes [67, 68]. Subiculum may act as a possible interface between the hippocampus and the neocortex during the consolidation of memories [69]. Interestingly, a relationship between cortical thinning in the subicular and entorhinal regions with the decline in the ability to encode new memories over time has been reported in mild cognitive impairment patients [70]. Then, the early reduction in the subicular neurons along with the axonal/synaptic damage might contribute to the altered neuronal network in the hippocampus and entorhinal cortex seen in AD.

ACKNOWLEDGMENTS

This work was supported by Fondo de Investigación Sanitaria (FIS), from Instituto de Salud Carlos III of Spain, through grants PI12/01431 (to AG) and PI12/01439 (to JV), and by CIBERNED (PI2010/08 and PI2013/01) to JV and AG. LT-E and ES-M were recipients of PhD fellowships (FPU) from Ministerio de Educacion, Cultura y Deportes (Spain). We thank Sanofi for the A β PP/PS1 model used in this study, and Mercedes Aneiros for her expert technical assistance. Antonia Gutierrez and Javier Vitorica are Co-Senior corresponding authors.

Authors' disclosures available online (<http://www.jalz.com/disclosures/view.php?id=2268>).

REFERENCES

- [1] Davies CA, Mann DM, Sumpter PQ, Yates PO (1987) A quantitative morphometric analysis of the neuronal and synaptic content of the frontal and temporal cortex in patients with Alzheimer's disease. *J Neurol Sci* **78**, 151-164.
- [2] Gomez-Isla T, Price JL, McKeel DW, Jr, Morris JC, Growdon JH, Hyman BT (1996) Profound loss of layer II entorhinal cortex neurons occurs in very mild Alzheimer's disease. *J Neurosci* **16**, 4491-4500.
- [3] Masliah E, Mallory M, Alford M, DeTeresa R, Hansen LA, McKeel DW Jr, Morris JC (2001) Altered expression of synaptic proteins occurs early during progression of Alzheimer's disease. *Neurology* **56**, 127-129.
- [4] Price JL, Ko AI, Wade MJ, Tsou SK, McKeel DW, Morris JC (2001) Neuron number in the entorhinal cortex and CA1 in preclinical Alzheimer disease. *Arch Neurol* **58**, 1395-1402.

- [5] Scheff SW, Price DA, Schmitt FA, Mufson EJ (2006) Hippocampal synaptic loss in early Alzheimer's disease and mild cognitive impairment. *Neurobiol Aging* **27**, 1372-1384.
- [6] Terry RD, Masliah E, Salmon DP, Butters N, DeTeresa R, Hill R, Hansen LA, Katzman R (1991) Physical basis of cognitive alterations in Alzheimer's disease: Synapse loss is the major correlate of cognitive impairment. *Ann Neurol* **30**, 572-580.
- [7] Kitazawa M, Medeiros R, Laferla FM (2012) Transgenic mouse models of Alzheimer disease: Developing a better model as a tool for therapeutic interventions. *Curr Pharm Des* **18**, 1131-1147.
- [8] Laferla FM, Green KN (2012) Animal models of Alzheimer disease. *Cold Spring Harb Perspect Med* **2**, pii: a006320.
- [9] Platt TL, Reeves VL, Murphy MP (2013) Transgenic models of Alzheimer's disease: Better utilization of existing models through viral transgenesis. *Biochim Biophys Acta* **1832**, 1437-1448.
- [10] Schaeffer EL, Figueiro M, Gattaz WF (2011) Insights into Alzheimer disease pathogenesis from studies in transgenic animal models. *Clinics (Sao Paulo)* **66**(Suppl 1), 45-54.
- [11] Amaral DG, Witter MP (1989) The three-dimensional organization of the hippocampal formation: A review of anatomical data. *Neuroscience* **31**, 571-591.
- [12] O'Mara S (2005) The subiculum: What it does, what it might do, and what neuroanatomy has yet to tell us. *J Anat* **207**, 271-282.
- [13] O'Mara SM, Commins S, Anderson M, Gigg J (2001) The subiculum: A review of form, physiology and function. *Prog Neurobiol* **64**, 129-155.
- [14] Ball MJ (1977) Neuronal loss, neurofibrillary tangles and granulovacuolar degeneration in the hippocampus with ageing and dementia. A quantitative study. *Acta Neuropathol* **37**, 111-118.
- [15] Bobinski M, Wegiel J, Tarnawski M, Bobinski M, Reisberg B, de Leon MJ, Miller DC, Wisniewski HM (1997) Relationships between regional neuronal loss and neurofibrillary changes in the hippocampal formation and duration and severity of Alzheimer disease. *J Neuropathol Exp Neurol* **56**, 414-420.
- [16] Davies DC, Horwood N, Isaacs SL, Mann DM (1992) The effect of age and Alzheimer's disease on pyramidal neuron density in the individual fields of the hippocampal formation. *Acta Neuropathol* **83**, 510-517.
- [17] Kril JJ, Patel S, Harding AJ, Halliday GM (2002) Neuron loss from the hippocampus of Alzheimer's disease exceeds extracellular neurofibrillary tangle formation. *Acta Neuropathol* **103**, 370-376.
- [18] Simic G, Kostovic I, Winblad B, Bogdanovic N (1997) Volume and number of neurons of the human hippocampal formation in normal aging and Alzheimer's disease. *J Comp Neurol* **379**, 482-494.
- [19] West MJ (1993) Regionally specific loss of neurons in the aging human hippocampus. *Neurobiol Aging* **14**, 287-293.
- [20] West MJ, Kawas CH, Martin LJ, Troncoso JC (2000) The CA1 region of the human hippocampus is a hot spot in Alzheimer's disease. *Ann N Y Acad Sci* **908**, 255-259.
- [21] West MJ, Kawas CH, Stewart WF, Rudow GL, Troncoso JC (2004) Hippocampal neurons in pre-clinical Alzheimer's disease. *Neurobiol Aging* **25**, 1205-1212.
- [22] Bobinski M, Wegiel J, Wisniewski HM, Tarnawski M, Bobinski M, Reisberg B, de Leon MJ, Miller DC (1996) Neurofibrillary pathology—correlation with hippocampal formation atrophy in Alzheimer disease. *Neurobiol Aging* **17**, 909-919.
- [23] Franko E, Joly O (2013) Evaluating Alzheimer's disease progression using rate of regional hippocampal atrophy. *PLoS One* **8**, e71354.
- [24] Baglietto-Vargas D, Moreno-Gonzalez I, Sanchez-Varo R, Jimenez S, Trujillo-Estrada L, Sanchez-Mejias E, Torres M, Romero-Acebal M, Ruano D, Vizuete M, Vitorica J, Gutierrez A (2010) Calretinin interneurons are early targets of extracellular amyloid-beta pathology in PS1/AbetaPP Alzheimer mice hippocampus. *J Alzheimers Dis* **21**, 119-132.
- [25] Ramos B, Baglietto-Vargas D, Del Rio JC, Moreno-Gonzalez I, Santa-Maria C, Jimenez S, Caballero C, Lopez-Tellez JF, Khan ZU, Ruano D, Gutierrez A, Vitorica J (2006) Early neuropathology of somatostatin/NPY GABAergic cells in the hippocampus of a PS1xAPP transgenic model of Alzheimer's disease. *Neurobiol Aging* **27**, 1658-1672.
- [26] Moreno-Gonzalez I, Baglietto-Vargas D, Sanchez-Varo R, Jimenez S, Trujillo-Estrada L, Sanchez-Mejias E, Del Rio JC, Torres M, Romero-Acebal M, Ruano D, Vizuete M, Vitorica J, Gutierrez A (2009) Extracellular amyloid-beta and cytotoxic glial activation induce significant entorhinal neuron loss in young PS1(M146L)/APP(751SL) mice. *J Alzheimers Dis* **18**, 755-776.
- [27] Jimenez S, Baglietto-Vargas D, Caballero C, Moreno-Gonzalez I, Torres M, Sanchez-Varo R, Ruano D, Vizuete M, Gutierrez A, Vitorica J (2008) Inflammatory response in the hippocampus of PS1M146L/APP751SL mouse model of Alzheimer's disease: Age-dependent switch in the microglial phenotype from alternative to classic. *J Neurosci* **28**, 11650-11661.
- [28] Killiany RJ, Hyman BT, Gomez-Isla T, Moss MB, Kikinis R, Jolesz F, Tanzi R, Jones K, Albert MS (2002) MRI measures of entorhinal cortex vs hippocampus in preclinical AD. *Neurology* **58**, 1188-1196.
- [29] Pennanen C, Kivipelto M, Tuomainen S, Hartikainen P, Hanninen T, Laakso MP, Hallikainen M, Vanhanen M, Nissinen A, Helkala EL, Vainio P, Vanninen R, Partanen K, Soininen H (2004) Hippocampus and entorhinal cortex in mild cognitive impairment and early AD. *Neurobiol Aging* **25**, 303-310.
- [30] Jimenez S, Torres M, Vizuete M, Sanchez-Varo R, Sanchez-Mejias E, Trujillo-Estrada L, Carmona-Cuenca I, Caballero C, Ruano D, Gutierrez A, Vitorica J (2011) Age-dependent accumulation of soluble amyloid beta (A β) oligomers reverses the neuroprotective effect of soluble amyloid precursor protein-alpha (sAPP(alpha)) by modulating phosphatidylinositol 3-kinase (PI3K)/Akt-GSK-3beta pathway in Alzheimer mouse model. *J Biol Chem* **286**, 18414-18425.
- [31] Ding SL (2013) Comparative anatomy of the prosubiculum, subiculum, presubiculum, postsubiculum, and parasubiculum in human, monkey, and rodent. *J Comp Neurol* **521**, 4145-4162.
- [32] Apostolova LG, Dutton RA, Dinov ID, Hayashi KM, Toga AW, Cummings JL, Thompson PM (2006) Conversion of mild cognitive impairment to Alzheimer disease predicted by hippocampal atrophy maps. *Arch Neurol* **63**, 693-699.
- [33] Falke E, Nissanov J, Mitchell TW, Bennett DA, Trojanowski JQ, Arnold SE (2003) Subicular dendritic arborization in Alzheimer's disease correlates with neurofibrillary tangle density. *Am J Pathol* **163**, 1615-1621.
- [34] Hyman BT, Van Hoesen GW, Damasio AR, Barnes CL (1984) Alzheimer's disease: Cell-specific pathology isolates the hippocampal formation. *Science* **225**, 1168-1170.
- [35] La JR, Perrotin A, de LS, V, Egret S, Doeuvre L, Belliard S, Eustache F, Desgranges B, Chetelat G (2013) Hippocampal subfield volumetry in mild cognitive impairment, Alzheimer's

- disease and semantic dementia. *Neuroimage Clin* **3**, 155-162.
- [36] Van Hoesen GW, Hyman BT (1990) Hippocampal formation: Anatomy and the patterns of pathology in Alzheimer's disease. *Prog Brain Res* **83**, 445-457.
- [37] Davies DC, Wilmott AC, Mann DM (1988) Senile plaques are concentrated in the subicular region of the hippocampal formation in Alzheimer's disease. *Neurosci Lett* **94**, 228-233.
- [38] Eimer WA, Vassar R (2013) Neuron loss in the 5XFAD mouse model of Alzheimer's disease correlates with intraneuronal Abeta42 accumulation and Caspase-3 activation. *Mol Neurodegener* **8**, 2.
- [39] Oakley H, Cole SL, Logan S, Maus E, Shao P, Craft J, Guillozet-Bongaarts A, Ohno M, Disterhoft J, Van EL, Berry R, Vassar R (2006) Intraneuronal beta-amyloid aggregates, neurodegeneration, and neuron loss in transgenic mice with five familial Alzheimer's disease mutations: Potential factors in amyloid plaque formation. *J Neurosci* **26**, 10129-10140.
- [40] Blanchard V, Moussaoui S, Czech C, Touchet N, Bonici B, Planche M, Canton T, Jedidi I, Gohin M, Wirths O, Bayer TA, Langui D, Duyckaerts C, Tremp G, Pradier L (2003) Time sequence of maturation of dystrophic neurites associated with Abeta deposits in APP/PS1 transgenic mice. *Exp Neurol* **184**, 247-263.
- [41] Sanchez-Varo R, Trujillo-Estrada L, Sanchez-Mejias E, Torres M, Baglietto-Vargas D, Moreno-Gonzalez I, De C, V, Jimenez S, Ruano D, Vizuete M, Davila JC, Garcia-Verdugo JM, Jimenez AJ, Vitorica J, Gutierrez A (2012) Abnormal accumulation of autophagic vesicles correlates with axonal and synaptic pathology in young Alzheimer's mice hippocampus. *Acta Neuropathol* **123**, 53-70.
- [42] Paxinos G, Franklin KBJ (2008) *The Mouse Brain in Stereotaxic Coordinates*, Academic Press, New York.
- [43] Gundersen HJ, Bagger P, Bendtsen TF, Evans SM, Korbo L, Marcussen N, Moller A, Nielsen K, Nyengaard JR, Pakkenberg B (1988) The new stereological tools: Disector, fractionator, nucleator and point sampled intercepts and their use in pathological research and diagnosis. *APMIS* **96**, 857-881.
- [44] Schmitz C, Rutten BP, Pielen A, Schafer S, Wirths O, Tremp G, Czech C, Blanchard V, Multhaup G, Rezaie P, Korr H, Steinbusch HW, Pradier L, Bayer TA (2004) Hippocampal neuron loss exceeds amyloid plaque load in a transgenic mouse model of Alzheimer's disease. *Am J Pathol* **164**, 1495-1502.
- [45] Torres M, Jimenez S, Sanchez-Varo R, Navarro V, Trujillo-Estrada L, Sanchez-Mejias E, Carmona I, Davila JC, Vizuete M, Gutierrez A, Vitorica J (2012) Defective lysosomal proteolysis and axonal transport are early pathogenic events that worsen with age leading to increased APP metabolism and synaptic Abeta in transgenic APP/PS1 hippocampus. *Mol Neurodegener* **7**, 59.
- [46] Lee S, Sato Y, Nixon RA (2011) Primary lysosomal dysfunction causes cargo-specific deficits of axonal transport leading to Alzheimer-like neuritic dystrophy. *Autophagy* **7**, 1562-1563.
- [47] Nixon RA, Wegiel J, Kumar A, Yu WH, Peterhoff C, Cataldo A, Cuervo AM (2005) Extensive involvement of autophagy in Alzheimer disease: An immuno-electron microscopy study. *J Neuropathol Exp Neurol* **64**, 113-122.
- [48] Casas C, Sergeant N, Itier JM, Blanchard V, Wirths O, van der KN, Vingtdoux V, van de SE, Ret G, Canton T, Drobecq H, Clark A, Bonici B, Delacourte A, Benavides J, Schmitz C, Tremp G, Bayer TA, Benoit P, Pradier L (2004) Massive CA1/2 neuronal loss with intraneuronal and N-terminal truncated Abeta42 accumulation in a novel Alzheimer transgenic model. *Am J Pathol* **165**, 1289-1300.
- [49] Cohen RM, Rezai-Zadeh K, Weitz TM, Rentsendorj A, Gate D, Spivak I, Bholat Y, Vasilevko V, Glabe CG, Breunig JJ, Rakic P, Davtyan H, Agadjanyan MG, Kepe V, Barrio JR, Bannykh S, Szekely CA, Pechnick RN, Town T (2013) A transgenic Alzheimer rat with plaques, tau pathology, behavioral impairment, oligomeric abeta, and frank neuronal loss. *J Neurosci* **33**, 6245-6256.
- [50] Saul A, Sprenger F, Bayer TA, Wirths O (2013) Accelerated tau pathology with synaptic and neuronal loss in a novel triple transgenic mouse model of Alzheimer's disease. *Neurobiol Aging* **34**, 2564-2573.
- [51] Wright AL, Zinn R, Hohensinn B, Konen LM, Beynon SB, Tan RP, Clark IA, Abdipranoto A, Vissel B (2013) Neuroinflammation and neuronal loss precede Abeta plaque deposition in the hAPP-J20 mouse model of Alzheimer's disease. *PLoS One* **8**, e59586.
- [52] Ronnback A, Zhu S, Dillner K, Aoki M, Lilius L, Naslund J, Winblad B, Graff C (2011) Progressive neuropathology and cognitive decline in a single Arctic APP transgenic mouse model. *Neurobiol Aging* **32**, 280-292.
- [53] Martins IC, Kuperstein I, Wilkinson H, Maes E, Vanbrabant M, Jonckheere W, Van GP, Hartmann D, D'Hooge R, De SB, Schymkowitz J, Rousseau F (2008) Lipids revert inert Abeta amyloid fibrils to neurotoxic protofibrils that affect learning in mice. *EMBO J* **27**, 224-233.
- [54] De Felice FG, Wu D, Lambert MP, Fernandez SJ, Velasco PT, Lacor PN, Bigio EH, Jerecic J, Acton PJ, Shughrue PJ, Chen-Dodson E, Kinney GG, Klein WL (2008) Alzheimer's disease-type neuronal tau hyperphosphorylation induced by A beta oligomers. *Neurobiol Aging* **29**, 1334-1347.
- [55] Jin M, Shepardson N, Yang T, Chen G, Walsh D, Selkoe DJ (2011) Soluble amyloid beta-protein dimers isolated from Alzheimer cortex directly induce tau hyperphosphorylation and neuritic degeneration. *Proc Natl Acad Sci U S A* **108**, 5819-5824.
- [56] Decker H, Lo KY, Unger SM, Ferreira ST, Silverman MA (2010) Amyloid-beta peptide oligomers disrupt axonal transport through an NMDA receptor-dependent mechanism that is mediated by glycogen synthase kinase 3beta in primary cultured hippocampal neurons. *J Neurosci* **30**, 9166-9171.
- [57] Liu Y, Yoo MJ, Savonenko A, Stirling W, Price DL, Borchelt DR, Mamounas L, Lyons WE, Blue ME, Lee MK (2008) Amyloid pathology is associated with progressive monoaminergic neurodegeneration in a transgenic mouse model of Alzheimer's disease. *J Neurosci* **28**, 13805-13814.
- [58] Iwamoto N, Emson PC (1991) Demonstration of neurofibrillary tangles in parvalbumin-immunoreactive interneurons in the cerebral cortex of Alzheimer-type dementia brain. *Neurosci Lett* **128**, 81-84.
- [59] Takahashi H, Brasnjevic I, Rutten BP, van der KN, Perl DP, Bouras C, Steinbusch HW, Schmitz C, Hof PR, Dickstein DL (2010) Hippocampal interneuron loss in an APP/PS1 double mutant mouse and in Alzheimer's disease. *Brain Struct Funct* **214**, 145-160.
- [60] Bennett DA (2006) Postmortem indices linking risk factors to cognition: Results from the Religious Order Study and the Memory and Aging Project. *Alzheimer Dis Assoc Disord* **20**, S63-S68.
- [61] Kantarci K (2014) Molecular imaging of Alzheimer disease pathology. *AJNR Am J Neuroradiol*. doi: 10.3174/ajnr.A3847
- [62] Negash S, Bennett DA, Wilson RS, Schneider JA, Arnold SE (2011) Cognition and neuropathology in aging: Multidimen-

- sional perspectives from the Rush Religious Orders Study and Rush Memory And Aging Project. *Curr Alzheimer Res* **8**, 336-340.
- [63] Perrin RJ, Fagan AM, Holtzman DM (2009) Multimodal techniques for diagnosis and prognosis of Alzheimer's disease. *Nature* **461**, 916-922.
- [64] Price JL, Morris JC (1999) Tangles and plaques in nondemented aging and "preclinical" Alzheimer's disease. *Ann Neurol* **45**, 358-368.
- [65] Perez-Nievas BG, Stein TD, Tai HC, Dols-Icardo O, Scotton TC, Barroeta-Espar I, Fernandez-Carballo L, de Munain EL, Perez J, Marquie M, Serrano-Pozo A, Frosch MP, Lowe V, Parisi JE, Petersen RC, Ikonomic MD, Lopez OL, Klunk W, Hyman BT, Gomez-Isla T (2013) Dissecting phenotypic traits linked to human resilience to Alzheimer's pathology. *Brain* **136**, 2510-2526.
- [66] Trujillo-Estrada L, Jimenez S, De C, Torres V, Baglietto-Vargas M, Moreno-Gonzalez D, Navarro I, Sanchez-Varo V, Sanchez-Mejias R, Davila E, Vizuete JC, Gutierrez M, Vitorica A, J (2013) *In vivo* modification of Abeta plaque toxicity as a novel neuroprotective lithium-mediated therapy for Alzheimer's disease pathology. *Acta Neuropathol Commun* **1**, 73.
- [67] O'Mara S (2006) Controlling hippocampal output: The central role of subiculum in hippocampal information processing. *Behav Brain Res* **174**, 304-312.
- [68] O'Mara SM, Sanchez-Vives MV, Brotons-Mas JR, O'Hare E (2009) Roles for the subiculum in spatial information processing, memory, motivation and the temporal control of behaviour. *Prog Neuropsychopharmacol Biol Psychiatry* **33**, 782-790.
- [69] Craig S, Commins S (2006) The subiculum to entorhinal cortex projection is capable of sustaining both short- and long-term plastic changes. *Behav Brain Res* **174**, 281-288.
- [70] Burggren AC, Renner B, Jones M, Donix M, Suthana NA, Martin-Harris L, Ercoli LM, Miller KJ, Siddarth P, Small GW, Bookheimer SY (2011) Thickness in entorhinal and subicular cortex predicts episodic memory decline in mild cognitive impairment. *Int J Alzheimers Dis* **2011**, 956053.